The Plasma and Cytoplasmic Forms of Human Gelsolin Differ in Disulfide Structure†

Dingyi Wen,‡ Karen Corina,‡ E. Pingchang Chow,‡ Stephan Miller,‡ Paul A. Janmey,§ and R. Blake Pepinsky*,‡

Biogen, Inc., 14 Cambridge Center, Cambridge, Massachusetts 02142, and Program in Biological and Medical Science, Harvard Medical School, Boston, Massachusetts 02115

Received April 16, 1996⊗

ABSTRACT: Gelsolin is a widely distributed actin binding protein that regulates actin filament length. It exists in both an intracellular and an extracellular form that is derived from a single gene by alternative splicing. Both forms contain the six homologous domains that are responsible for function. Little is known regarding differences between the forms. We have used a combination of cysteine-specific modification with 4-vinylpyridine, HPLC peptide mapping methods, and mass spectrometry to analyze the disulfide structures of human plasma and cytoplasmic gelsolin. Of the five Cys residues in the human gelsolin sequence, all were present in the free thiol form in human cytoplasmic gelsolin, while only three of them were free thiols in the human plasma form. Cys residues 188 and 201 in domain 2 of plasma gelsolin were disulfide linked. Recombinant human plasma gelsolin that had been expressed intracellularly in *Escherichia coli* and as a secreted protein from Cos green monkey cells was also investigated. The *E. coli* product lacked the disulfide but could be converted to the plasma-like structure with mild oxidation while the mammalian product formed the correct disulfide prior to isolation. Structural differences were also detected by limited proteolysis with plasmin. The differences in proteolytic susceptibility were also due to perturbations in domain 2. These studies demonstrate that the intracellular and extracellular gelsolins are structurally distinct and suggest that at least some of the preparations of recombinant gelsolin that are being used to study structure/function may be improperly folded. The experiments also demonstrate a general method for the location of disulfide bonds in proteins.

Gelsolin is a member of a family of actin binding proteins including villin, severin, and fragmin that regulates actin filament length. This can occur by severing preexisting filaments, promoting filament formation from actin monomers through a nucleating activity, and/or capping the fast growing "barbed" end of filaments [Yin & Stossel, 1979; reviewed in Stossel et al. (1985) and Weeds and Maciver (1993)]. Intrinsic factors such as the actin concentration and the ratio of actin to actin binding protein are important variables that govern whether the filaments are growing or shrinking. Gelsolin activity also is regulated by calcium and phosphoinositides [reviewed by Yin (1987) and Janmey (1995)]. Recent data from mice lacking the gelsolin gene indicate diverse functions in hemostasis, inflammatory responses, and fibroblast responses (Witke et al., 1995), and it has been targeted as a potential therapeutic agent for the treatment of cystic fibrosis patients (Vasconcellos et al., 1994).

Natural gelsolin exists in two forms, plasma and cytoplasmic, that differ by alternative splicing (Kwiatkowski et al., 1986). Both forms contain a 730 amino acid core structure that is made up of six repeated domains. The putative domain boundaries are residues 30−149, 150−266, 267−389, 407−528, 529−634, and 635−755 (numbering based on the mature plasma gelsolin sequence; Way & Weeds, 1988). The six domains make up three distinct actin binding sites that have been localized within domains 1, 2, and 4 by limited proteolysis and cloning strategies (Kwiatkowski et al., 1989; Way et al., 1989; Pope et al., 1995). The plasma form contains a N-terminal extension of 25 amino acids of unknown function (Kwiatkowski et al., 1988). The X-ray crystal structure of a complex of gelsolin domain 1 and actin (McLaughlin et al., 1993) and solution NMR structures of domain 1 from villin (Markus et al., 1994) and domain 2 from severin (Schnuchel et al., 1995) have been recently reported. In these proteins, it is thought that each domain is independently folded but that the domains have similar tertiary structures (McLaughlin et al., 1993). Both plasma and cytoplasmic forms of human gelsolin contain five Cys residues, one each in domains 1, 3, and 6, and two in domain 2. The disulfide structure of human gelsolin is unknown, but in a recently published NMR structure for domain 2 from severin, the authors noted the presence of a disulfide bond (Schnuchel et al., 1995). The presence of a single disulfide in bovine plasma gelsolin, which contains seven Cys residues, has been inferred from studies with Ellman's reagent (Kilhoffer & Gerard, 1985).

The reason for the two forms of gelsolin is unknown. The sparsity of the cytoplasmic form and difficulty in isolating it free from actin have hampered a rigorous comparison of potential differences between the proteins. Typical purification methods rely on denaturants or chaotropes as part of the method, which may alter the properties of the protein. In one study where actin severing properties of cytoplasmic and plasma forms of human gelsolin were compared by microinjection into cells, the proteins displayed different activities (Huckriede et al., 1990), raising the possibility that

† P.A.J. is supported by NIH Grant HL54253 and CF Foundation Grant G957.

* To whom correspondence and reprint requests should be addressed. Telephone: (617) 679-2299 and -3310.

‡ Biogen, Inc.

§ Harvard Medical School.

⊗ Abstract published in *Advance ACS Abstracts,* July 15, 1996.

S0006-2960(96)00920-8 CCC: $12.00

structural differences might also exist. Since the oxidation−reduction states of intracellular and extracellular milieu are different (Hwang et al., 1992), we have tested for differences in the disulfide structure of cytoplasmic and plasma gelsolin.

Here, using peptide mapping and mass spectrometry to identify the Cys-containing peptides, we show that the cytoplasmic and plasma forms of gelsolin indeed are structurally distinct. We also found that recombinant plasma gelsolin that was expressed in *E. coli* lacked the disulfide but could be converted to the plasma-like structure with mild oxidation. The changes in disulfide structure tracked with differences in proteolytic susceptibility and provide the first definitive evidence for structural differences between plasma and cytoplasmic gelsolin.

EXPERIMENTAL PROCEDURES

Purification of Human Plasma Gelsolin. Gelsolin was purified from human plasma using a modified version of the published method for bovine gelsolin (Kurokawa et al., 1990). The gelsolin was precipitated from plasma using a 35−50% ammonium sulfate cut, dialyzed, and purified by DE52 anion-exchange chromatography as described. Gelsolin-containing fractions were identified by SDS−PAGE[1] and pooled. The product was further purified by cation-exchange chromatography on SP-Sepharose (Pharmacia). The pH of the eluate pool was lowered to 6.0 with MES and loaded onto a SP-Sepharose column that was equilibrated with 50 mM MES, pH 6.0. The column was washed with 50 mM MES, pH 6.0, and the gelsolin was eluted with 25 mM Tris-HCl, pH 7.5, and 180 mM NaCl. Typically about 1 mg of gelsolin was obtained from 50 mL of human plasma. The gelsolin was aliquoted and stored at −70 °C.

Purification of Human Cytoplasmic Gelsolin. Cytoplasmic gelsolin for disulfide analysis was purified from fresh platelets obtained from the American Red Cross within 5 days of isolation. Gelsolin−actin complexes were purified from the platelets by DNase I affinity chromatography. The platelets were washed as described by Kurth and Bryan (1984), lysed by sonication, and then applied to a DNase I affinity column following the method developed by Wang and Bryan (1981). The eluate was subjected to reversed-phase HPLC on a Vydac C_4 column. The column was developed with a 30 min 0−70% gradient of acetonitrile in 0.1% trifluoroacetic acid at a flow rate of 1.4 mL/min. The column effluent was monitored at 280 nm and 0.5 min fractions were collected. Gelsolin-containing fractions of >90% purity were identified by SDS−PAGE.

Purification of Recombinant Human Plasma Gelsolin from Escherichia coli. The plasma form of gelsolin was expressed in *E. coli* behind the P_L promotor. Cells in 50 mM Tris-HCl, pH 8.0, 30 mM NaCl, and 1 mM EDTA (1 part of wet cell weight to 9 parts of buffer) were lysed in a Manton gaulin and subjected to centrifugation for 1 h at 14000*g*. The supernatant was loaded onto a Q-Sepharose column equilibrated in the same buffer. The column was washed with 4 column volumes of the load buffer and then with 3 column volumes of the same buffer containing 100 mM NaCl. Gelsolin was eluted with 25 mM Tris-HCl, pH 8.0, 150 mM NaCl, and 1 mM EDTA. The gelsolin was diluted 1:1 with 25 mM Tris-HCl, pH 8.0, and 1 mM EDTA, and loaded onto a second Q-Sepharose column. The column was subjected to the same wash strategy except the second wash contained only 30 mM NaCl. The gelsolin was eluted with 25 mM Tris-HCl, pH 8.0, 75 mM NaCl, and 2 mM $CaCl_2$. The gelsolin was further purified on a SP-Sepharose column. The column was washed with 50 mM MES, pH 6.0, and then the gelsolin was eluted with 15 mM sodium phosphate, pH 7.5, and 300 mM NaCl. All columns were routinely loaded at 10−20 mg of total protein/mL of resin with an overall recovery of approximately 1 g of gelsolin/kg of cells (wet weight).

Purification of Recombinant Human Plasma Gelsolin from Cos 7 Cells. The human plasma gelsolin gene in a CDM8 expression plasmid (Kwiatkowski & Yin, 1989) was transfected into Cos 7 cells by electroporation. After 24 h, the cells were transferred to serum-free media. After an additional 72 h, the conditioned medium was filtered (0.2 μm), concentrated by ultrafiltration in an Amicon stirred cell, and dialyzed overnight against 25 mM Tris-HCl, pH 8.0, 45 mM NaCl, and 1 mM EDTA. The dialyzed material was subjected to the same DE52/SP-Sepharose purification protocol described above for natural plasma gelsolin. Four milligrams of gelsolin was purified from 2 L of cell culture media.

Alkylation of Gelsolin. Samples containing about 60 μg of gelsolin in 0.1 mL of 6 M guanidine hydrochloride in the presence or absence of 50 mM dithiothreitol were treated with 500 mM 4-vinylpyridine for 2−3 h at room temperature. Alkylated gelsolin was recovered by precipitation with 40 volumes of cooled ethanol (Pepinsky, 1991). The solution was stored at −20 °C for 1 h and then centrifuged at 14000*g* for 8 min at 4 °C. The supernatant was discarded and the protein was stored at −20 °C.

Peptide Mapping. Alkylated gelsolin (0.5 mg/mL in 20 mM Tris-HCl, pH 7.5) was digested with endo Asp-N (Calbiochem) at an enzyme to gelsolin ratio of 1:60 (w/w) or with endo Lys-C (Wako Pure Chemical Industries, Ltd.) at a 1:25 ratio. Digests were conducted at room temperature for 8 h with endo Asp-N or for 24 h with endo Lys-C. The reactions were stopped by acidification with 10 μL of 25% trifluoroacetic acid and analyzed by reversed-phase HPLC on a 2.1 mm × 25 cm Vydac C_{18} column. The column was developed with a 180 min gradient (0−90% acetonitrile) in 0.1% trifluoroacetic acid at a flow rate of 0.2 mL/min. The absorbance of the eluate was monitored using a Waters Model 991M photodiode array detector. Individual peaks were manually collected for mass and/or sequence analysis. Prior to injection, solid guanidinium chloride was added into the peptide solutions to a concentration of 6 M to dissolve insoluble material.

Titration of Thiol Groups. Thiol groups of native and denatured (in 6 M guanidine hydrochloride) gelsolin at 1−3 mg/mL were assayed with Ellman's reagent [5,5′-dithiobis-(2-nitrobenzoic acid)] by monitoring absorbance at 412 nm (Creighton, 1990). For denatured samples, absorbance maxima were reached after 4 min. Moles of free −SH were calculated either against a standard curve of reduced glutathione or from the molar extinction coefficient of thionitrobenzoate (ϵ_{412} = 13 700/(M cm) in 6 M guanidine hydrochloride and 14 150 in its absence).

[1] Abbreviations: endo Asp-N, endoprotease Asp-N; HPLC, high-performance liquid chromatography; endo Lys-C, endoprotease Lys-C; PE-Cys, [2-(4-pyridyl)ethyl]cysteine; MES, 4-morpholineethanesulfonic acid; PAGE, polyacrylamide gel electrophoresis.

Mass Determination. The molecular masses of peptides were determined by matrix-assisted laser desorption mass spectroscopy on a Finnigan LaserMat mass spectrometer using α-cyano-4-hydroxycinnamic acid as the matrix. All spectra were calibrated against internal standards.

Limited Proteolysis of Gelsolin with Plasmin. Human plasmin was obtained from Sigma (Catalogue No. P-4895). The protease was suspended at 1 mg/mL in water, aliquoted, and stored at −20 °C. Typically 10 μg of gelsolin in 20 μL of 25 mM Tris-HCl, pH 8.0, and 100 mM NaCl was incubated for 60 min at 37 °C with 0.6 μg of plasmin. Samples were treated with electrophoresis sample buffer and subjected to SDS−PAGE on a 10−20% gradient gel from Integrated Separation Systems. Each test sample was analyzed in the presence of 5 mM EDTA, with 2 mM $CaCl_2$ or with no addition.

For analysis of cytoplasmic gelsolin, a modified version of the method was developed in which the gelsolin was cleaved with plasmin while immobilized on 2C4-Sepharose. The anti-gelsolin 2C4 monoclonal antibody (Sigma) (Chaponnier et al., 1986) was purified on protein A−Sepharose and conjugated to CNBr−Sepharose 4B at 2 mg of antibody/mL of resin. Gelsolin samples (0.5 mL, 40 μg/mL) in 50 mM Tris-HCl, pH 7.5, 150 mM NaCl, 1 mM EDTA, and 0.1% Tween-20 were incubated with 20 μL of 2C4-Sepharose with continuous agitation at 4 °C for 1 h. The beads were collected by centrifugation, washed with 0.5 mL of 20 mM Tris-HCl, pH 7.1, 150 mM NaCl, 5 mM $MgCl_2$, 5 mM ATP, and 1 mM EGTA (1 h at ambient temperature with agitation), and treated with plasmin (1 h at 37 °C with agitation in 0.5 mL of 100 mM Tris-HCl, pH 7.5, and 0.5 mM $CaCl_2$). Gelsolin was released from the beads by incubation with electrophoresis sample buffer for 10 min at room temperature. Solution controls were run in which the gelsolin was treated with excesses of antibody or actin. For these tests, gelsolin (0.1 mg/mL) in 5 mM triethanolamine, pH 7.5, 100 mM KCl, 2 mM $MgCl_2$, 0.2 mM $CaCl_2$, and 0.5 mM ATP was incubated at ambient temperature for 1 h alone or in the presence of actin or 2C4 antibody and then subjected to plasmin digestion. Rabbit skeletal muscle actin was polymerized to F-actin immediately prior to use.

Glutathione-Induced Oxidation. *E. coli*-derived recombinant gelsolin in 25 mM Tris-HCl, pH 8.0, 2 mM $CaCl_2$, and 50 mM NaCl was incubated overnight at 4 °C in the presence or absence of 2 mM oxidized glutathione. The samples were treated with 4-vinylpyridine and subjected to peptide mapping with both endo Asp-N and endo Lys-C.

RESULTS

Determination of the Cys Oxidation State of Human Plasma Gelsolin. Human plasma gelsolin was purified from natural and recombinant sources using a modification of the calcium-dependent elution protocol published by Kurokawa et al. (1990) for bovine plasma gelsolin. The final product was >95% pure by SDS−PAGE and contained a single major band with apparent mass of 85 kDa (Figure 1, lanes a−d). Free thiol content was determined by reaction with 5,5′-dithiobis(2-nitrobenzoic acid) (Ellman's reagent) under native and denaturing conditions. The appearance of thionitrobenzoate was monitored at 412 nm. Recombinant gelsolin from *E. coli* contained 5.0 ± 0.1 mol of SH groups/mol of protein under denaturing conditions while the natural and

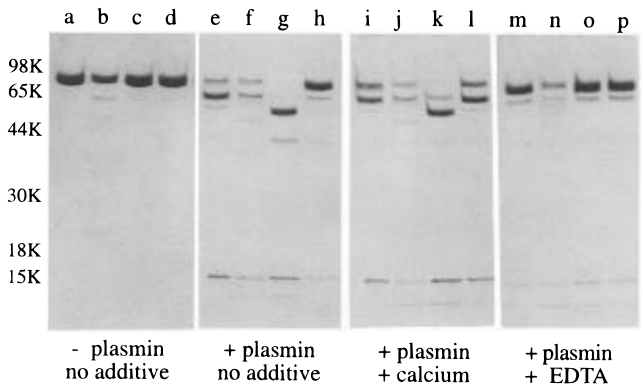

FIGURE 1: Analysis of the proteolytic susceptibility of plasma gelsolin by SDS−PAGE. Preparations of human plasma gelsolin alone (lanes a−d) or after treatment with plasmin (lanes e−p) were analyzed by SDS−PAGE. The proteins (3 μg/lane) were stained with Coomassie blue. Lanes a, e, i, and m, natural plasma gelsolin purified as described in Experimental Procedures. Lanes b, f, j, and n, natural plasma gelsolin purified by the one-step elution method. Lanes c, g, k, and o, recombinant plasma gelsolin from *E. coli*. Lanes d, h, l, and p, recombinant plasma gelsolin from Cos cells. The positions of molecular weight standards are indicated at the left of the figure.

the Cos-derived product contained only 3.0 ± 0.2 mol of SH group/mol of protein. Since a theoretical value of 5 would be expected if all the Cys residues were free, this result indicated the presence of a disulfide in the natural product. The same samples contained less than 0.1 mol of SH/mol of protein in the native, undenatured state.

Since many groups have worked with recombinant human plasma gelsolin and the methods for expression and purification are similar to what we employed (Way et al., 1989), it was unlikely that the product would be inactive for actin severing activity. Indeed, the recombinant and natural preparations of gelsolin displayed similar levels of actin severing assay when assayed with millimolar amounts of calcium present, reflecting concentrations which are routinely used to evaluate activity. Interestingly, when the products were tested side by side at low calcium concentration over a range of calcium concentrations, the natural gelsolin was more active than the recombinant, suggesting that differences in the disulfide structure impact function (data not shown). In this paper we have focused on biochemically defining the structural differences between the natural and recombinant products and have extended these analysis to evaluation of cytoplasmic gelsolin. A detailed evaluation of the functional differences between natural and recombinant gelsolin is presented elsewhere (P. Allen and P. Janmey, manuscript in preparation).

Analysis of the Disulfide Structure of Plasma Gelsolin by Peptide Mapping. The plasma gelsolin sequence contains Cys residues at positions 93, 188, 201, 304, and 645. A peptide mapping strategy was used to assess the disulfide structure of plasma gelsolin. Recombinant gelsolin from *E. coli* was pyridylethylated with 4-vinylpyridine and subjected to peptide mapping with endo Asp-N. Digests were analyzed by reversed-phase HPLC on a C_{18} column. Endo Asp-N was selected as the cleavage enzyme because it was expected to generate peptides that contain only one Cys residue. Figure 2 (left panel) shows the peptide map from an 8 h digest at 214, 254, and 280 nm. A time course study of the digestion showed no major changes in the HPLC profile between 2 and 16 h (data not shown). The gelsolin sequence

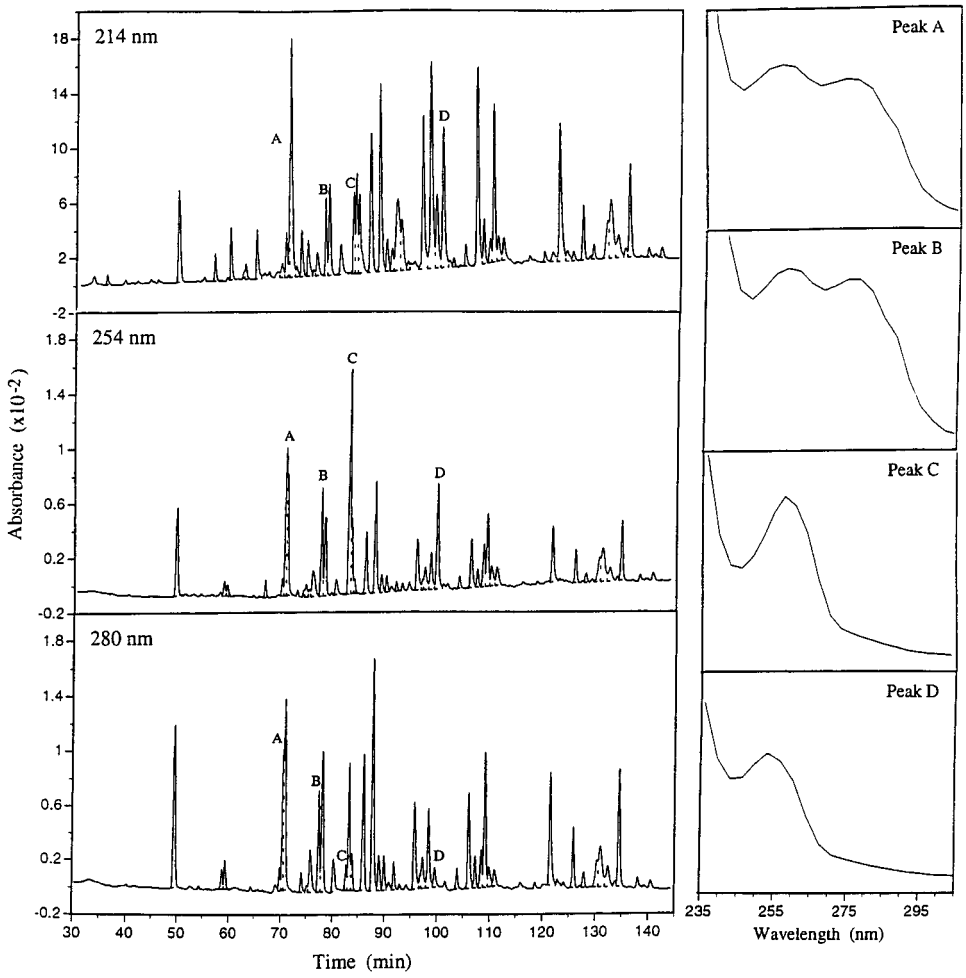

FIGURE 2: Identification of PE-Cys peptides in endo Asp-N digests of recombinant gelsolin. Recombinant gelsolin from *E. coli* was digested with endo Asp-N and subjected to peptide mapping by reversed-phase HPLC on a C_{18} column. Elution profiles at 214, 254, and 280 nm are shown. PE-Cys-containing peptides are denoted as peaks A−D. UV absorption spectra for the peaks are shown at the right of the figure. The presence of PE-Cys and of Trp/Tyr are indicated by respective absorption maxima at 254 and 280 nm.

Table 1: Sequences and Molecular Masses of Cys-Containing Endo Asp-N Peptides[a]

peak	residue no.	sequence (**J** = pyridylethyl-Cys)	MH^+ calcd	MH^+ found
A	192−208	DLGNNIHQW**J**GSNSNRY[b]	2083	2083
B	84−95	DLHYWLGNE**J**SQ	1570	1571
C	187−191 or 303−307	D**J**FIL	715	719
D	636−664	DAHPPRLFA**J**SNKIGRFVIEEVPGELMQE	3389	3409
E	187−191 or 303−307	DCFIL |	2589	2589
	192−208	DLGNNIHQWCGSNSNRY		

[a] Peaks A−D were found in pyridylethylated recombinant gelsolin from *E. coli* and in all reduced preparations of gelsolin. Peaks B−E were found in pyridylethylated natural gelsolin and the recombinant product from Cos cells. [b] The peak A peptide was generated as a result of cleavage at Glu^{209}. The expected endo Asp-N cleavage peptide was DLGNNIHQW**J**GSNSNRYERLKATQVSKGIR (residues 192−221: $MH^+ = 3551$).

contains 46 Asp residues, and after optimization of the gradient, around 40 major peaks could be detected from the digest.

Pyridylethyl-Cys (PE-Cys) has a maximum absorption at 254 nm, which can be used to identify PE-Cys-containing peptides directly from spectral data. Endo Asp-N digests of reduced and alkylated gelsolin should contain five Cys-containing peptides; however, since two of them have identical sequences, only four peaks were expected. Indeed, four PE-Cys peptide peaks were identified (peaks A−D, Figure 2). Two of these (peaks A and B) also had absorbance maxima at 280 nm, indicating the presence of aromatic residues. PE-Cys-containing peptides were further characterized by mass spectrometry. Peak assignments for the PE-Cys-containing peptides are shown in Table 1. The 254 nm absorbance for peak C (Figure 2) is twice that of the other PE-Cys-containing peptides (see peaks A and D) due to the presence of two copies of the peptide per mole of gelsolin. The height of peak B is variable because of partial cleavage at Glu^{92}. The peptide maps generated from samples with or without reduction were essentially identical, verifying that the five Cys residues in the recombinant gelsolin from *E. coli* are fully reduced (only data for the unreduced sample are shown).

When natural plasma gelsolin was subjected to the same analysis, the endo Asp-N peptide map was very similar to the profile seen with recombinant gelsolin. The major differences occurred in the region of the disulfide-containing

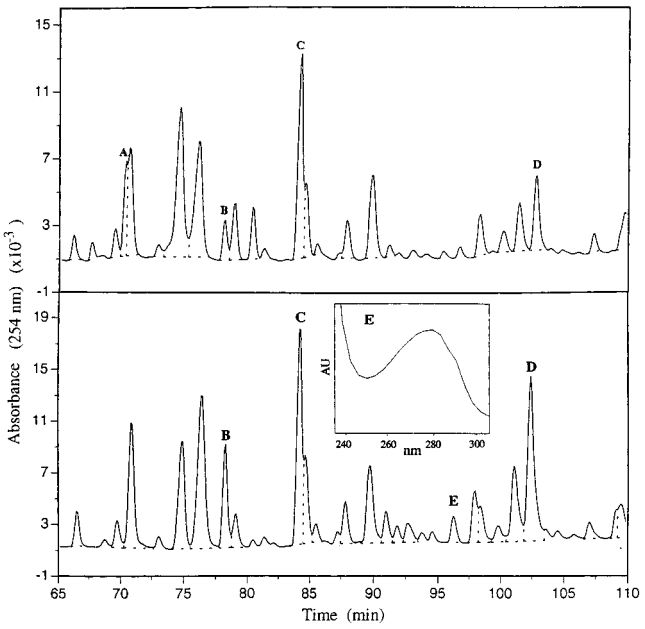

FIGURE 3: Comparison of endo Asp-N digests of recombinant and natural plasma gelsolin. Partial HPLC elution profiles of endo Asp-N digests of unreduced, pyridylethylated preparations of natural (lower panel) and recombinant gelsolin from *E. coli* (upper panel) were monitored at 254 nm. The four PE-Cys-containing peaks are indicated (A−D). UV spectra of PE-Cys-containing peaks B−D from natural gelsolin were essentially identical to those in Figure 2 for recombinant gelsolin. Inset: UV absorption spectrum of peak E, which contains the Cys^{188}−Cys^{201} disulfide.

peptides. The lower panel of Figure 3 shows an expanded region of the map from 65 to 110 min in order to better highlight the differences. The corresponding region from the map of recombinant gelsolin from *E. coli* is shown in the upper panel. Peak A is absent from the cleavage profile of natural gelsolin, and peak C is reduced in height relative to peaks B and D. The peptide map of natural gelsolin also contains an extra peak (peak E). The observed molecular mass ($MH^+ = 2589$) of peak E is consistent with that of a disulfide-linked peptide which is made up of the missing peak A and peak C components (see Table 1). Such a product would have a calculated MH^+ of 2589 and an absorption maximum at 280 nm due to aromatic residues. N-Terminal sequence analysis of peak E confirmed the presence of the two expected peptides.

Since the DCFIL peptide occurs twice in the gelsolin sequence (residues 187−191 and 303−307), two possibilities existed for the disulfide in plasma gelsolin: an intradomain 2 linkage between Cys^{188} and Cys^{201} or an interdomain linkage between Cys^{201} in domain 2 with Cys^{304} in domain 3. To distinguish between these possibilities, gelsolin was also subjected to peptide mapping with endo Lys-C, in which Cys^{188} and Cys^{304} are located in unique peptides. The gelsolin sequence has 45 potential endo Lys-C cleavage sites and should generate only four Cys-containing peptides, since Cys^{188} and Cys^{201} are in the same endo Lys-C fragment. Figure 4 shows the peptide map for pyridylethylated recombinant gelsolin from *E. coli* after 24 h of digestion. Shorter digestion times were tested but were inadequate due to incomplete cleavage (data not shown). Five PE-Cys-containing peptides were detected (labeled peaks F, G1, G2, H1, and H2 in Figure 4). Peak assignments based on absorption and mass spectra are shown in Table 2. Two of the peptides (G1 and H2) were partials resulting from

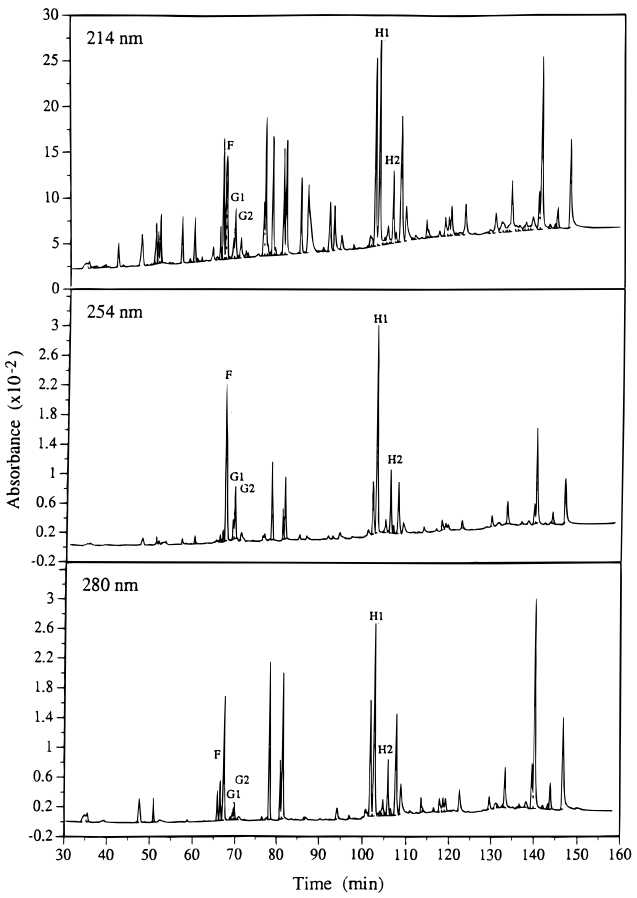

FIGURE 4: Identification of PE-Cys peptides in endo Lys-C digests of recombinant plasma gelsolin. The HPLC elution profiles from an endo Lys-C digest of unreduced, pyridylethylated, recombinant gelsolin from *E. coli* at 214, 254, and 280 nm are shown. The lettered peaks denote PE-Cys-containing peptides as indicated by UV maxima at 254 nm (data not shown).

incomplete cleavage at Lys residues. The three other peptides were as expected. The large Cys^{93} containing peptide corresponding to residues 73−135 was not detected, presumably due to irreversible binding to the C_{18} column.

A comparison of the endo Lys-C peptide maps of unreduced, PE-labeled, natural gelsolin (Figure 5, middle panel) and reduced, PE-labeled, natural plasma gelsolin (Figure 5, upper panel) revealed the loss of peaks H1 and H2 and the presence of a new peak (peak J) in the unreduced product. The absorbance spectrum of peak J contained a single absorbance maximum at 280 nm, indicating the presence of aromatic groups (data not shown). Mass spectral data for peak J ($MH^+ = 5340$) agreed with the theoretical mass ($MH^+ = 5338$) of the disulfide-linked peptide resulting from the intradomain 2 disulfide. The identity of peak J was further confirmed by N-terminal sequencing. As expected, only the one peptide sequence GRRVVRA... was obtained. The alternative interdomain disulfide structure would have resulted in a complex series of products due to partial proteolytic cleavage products with masses of 7160, 7032, 9117, and 9246 Da (see Table 2), and two peptide sequences would have been seen in N-terminal sequencing. Since the presence of peak H1 or J was a direct indication of the oxidation state of gelsolin, we used the peak J/peak J + H1 ratio as a measure of the amount of gelsolin containing the Cys^{188}−Cys^{201} disulfide, which proved to be a very sensitive assay for evaluating its oxidation state (see below).

Table 2: Sequences and Molecular Masses of Cys-Containing Endo Lys-C Peptides

peak	residue no.	sequence (**J** = pyridylethyl-Cys)[a]	MH^+ calcd	MH^+ found
F	301−311	SED**J**FILDHGK	1370	1370
G1	634−648	KMDAHPPRLFA**J**SNK	1822	1822
G2	635−648	MDAHPPRLFA**J**SNK	1693	1693
H1	167−212	GRRVVRATEVPVSWESFNNGD**J**FILDLGNNIHQW**J**GSNSNRYERLK	5550	5549
H2	151−212	HVVPNEVVVQRLFQVKGRRVVRATEVPVSWESFNNGD**J**FILDLGNNIHQW**J**GSNSNRYERLK	7424	7423
J[b]	167−212	GRRVVRATEVPVSWESFNNGDCFILDLGNNIHQWCGSNSNRYERLK	5338	5340

[a] The endo Lys-C peptide containing Cys^{93} (residues 73−135, TVQLRNGNLQYDLHYWLGNE**J**SQDESGAAAIFTVQLDDYLNGRAVQHREVQGFESATFLGYFK) was not detected in the peptide map. [b] The theoretical sequence for the interchain disulfide peptide containing the various combinations of H1/H2 and G1/G2 would have masses of 7160, 7032, 9117, and 9246.

(HVVPNEVVVQRLFQVK)GRRVVRATEVPVSWESFNNGDJFILDLGNNIHQWCGSNSNRYERLK

(K)KMDAHPPRLFACSNK

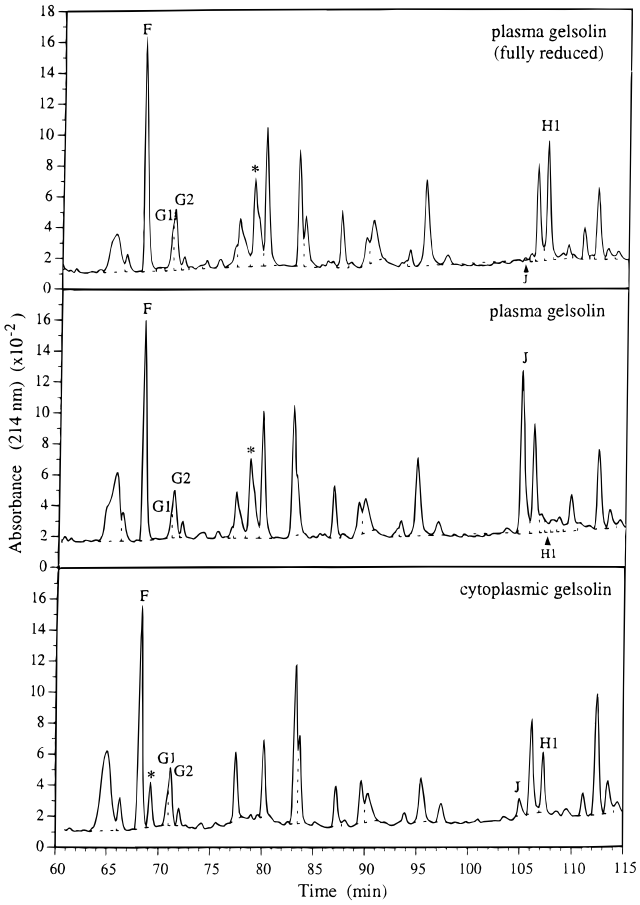

FIGURE 5: Comparisons of endo Lys-C digests of natural plasma and cytoplasmic gelsolin. Partial HPLC elution profiles from endo Lys-C digests of reduced, pyridylethylated, natural plasma gelsolin (upper panel), unreduced, pyridylethylated, natural gelsolin (middle panel), and pyridylethylated cytoplasmic gelsolin (lower panel) monitored at 214 nm are shown. Peaks F, G1, and G2 are as described in Figure 4 and have been identified in Table 2. Asterisks denote N-terminal endo Lys-C peptides from cytoplasmic and plasma gelsolin.

Analysis of the Disulfide Structure of Cytoplasmic Gelsolin. The disulfide structure of cytoplasmic gelsolin was also assessed by peptide mapping. Results from this study are shown in the lower panel of Figure 5. The pattern of PE-Cys-containing peptides resembles that of recombinant gelsolin from *E. coli* in that all of the expected Cys-containing peptides were detected, indicating that the five Cys residues in cytoplasmic gelsolin exist as free thiols. A small peak J component, representing about 20% of the product, was observed in the map of cytoplasmic gelsolin; however, we presume that this was generated during the purification by oxidation (discussed below; see Table 3). The peaks marked with asterisks in Figure 5 contained the predicted N-terminal peptides of cytoplasmic and plasma gelsolin (plasma gelsolin contains a 25 amino acid extension at its N-terminus). Their identities were confirmed by mass spectrometry (data not shown).

Table 3: Quantitation of Peptide Mapping Data[a]

sample	peak J/peaks J + H1 (%)
natural plasma gelsolin	>95
natural plasma gelsolin (reduced)	<5
cytoplasmic gelsolin	24
cytoplasmic gelsolin (+24 h dialysis)	40
E. coli-derived gelsolin	<5
E. coli-derived gelsolin (oxidized)	>95
E. coli-derived gelsolin (+24 h dialysis)	42
Cos-derived gelsolin	>92

[a] The relative amounts of Cys^{188}−Cys^{201} in the various preparations of gelsolin indicated above were quantified from endo Lys-C peptide maps. Values indicated reflect amounts of peak J relative to peak J + peak H1 based on peak height.

The relevant sequences from different species of gelsolin and other actin severing proteins such as severin, villin, and fragmin that are homologous with domain 2 are shown in Figure 6. Only mouse and pig gelsolin have the two Cys residues seen in human gelsolin. Lobster, fruit fly, and frog gelsolin as well as villin, severin, and fragmin are missing one or both of the Cys residues (severin discussed in detail below). Thus these related proteins already exist in forms that evolved with and without the disulfide.

Detection of Structural Differences between Natural and Recombinant Forms of Human Plasma Gelsolin by Limited Proteolysis. The differences in the disulfide structure of natural and recombinant forms of plasma gelsolin raised the possibility that more significant structural differences might exist. To test this possibility, samples were evaluated by CD and limited proteolysis. The CD spectra were very similar, indicating that there were no gross changes in structure. In contrast, the samples differed dramatically in their susceptibility to proteolysis. Many proteases could distinguish between the natural and recombinant products. Figure 1 shows the results from a study with plasmin. Under limiting digestion conditions, the major cleavage product of natural plasma gelsolin was a 70 kDa fragment (Figure 1, lane e) while the major cleavage product for recombinant gelsolin from *E. coli* was a 65 kDa fragment (lane g).

HUMAN GELSOLIN	176	**VP**VSWESFNN**GDCFIL**DLGNNIHQ**WCG**SNSNRYERL**KA**	213
PIG GELSOLIN	160	**VP**VSWESFNR**GDCFIL**DLGNDIYQ**WCG**SNSNRYERL**KA**	197
MOUSE GELSOLIN	152	**VP**VSWDSFNN**GDCFIL**DLGNNIYQ**WCG**SGSNKFERL**KA**	189
LOBSTER GELSOLIN	148	**V**EVGVGSMNK**GDCFIL**DCGSQVYA**YMG**PSSRKMDRL**KA**	185
FRUIT FLY GELSOLIN	200	**V**NLSVSSMNT**GDCFLL**DAGSDIYV**YVG**SQAKRVEKL**KA**	237
FROG GELSOLIN	237	**V**DNTASNLNSN**DAFVL**TTPSASYL**WVG**QGSTNVEKNG**A**	274
SEVERIN	177	**VP**LATSSLNS**GDCFLL**DAGLTIYQ**FNG**SKSSPQEKN**KA**	214
VILLIN	152	**V**EMSWKSFNL**GDVFLL**DLGQLIIQ**WNG**PESNRAERL**RA**	189
FRAGMIN	169	**VP**KTYKSLNS**GDVFVL**DAGKTVIQ**WNG**AKAGLLEKV**KA**	206

FIGURE 6: Comparison of sequences for the Cys^{188}−Cys^{201} region from various gelsolins and related proteins. Alignments of homologous sequences in domain 2 of plasma gelsolins from human (Bazari et al., 1988), pig (Way & Weeds, 1988), fruit fly (Heintzelman et al., 1993), and African clawed frog (Ankenbauer et al., 1988), mouse cytoplasmic gelsolin (Dieffenbach et al., 1989), American lobster gelsolin (Lueck et al., 1994), severin from *Dictyostelium* (Bazari et al., 1988), chicken intestinal villin (Bazari et al., 1988), and fragmin from *Physarium polycephalum* (Bazari et al., 1988) are shown. Bold residues indicate invariant amino acids or reflect conservative substitutions.

Since calcium is known to induce a structural change in gelsolin (Kilhoffer & Gerard, 1985; Reid et al., 1993), we next tested if calcium affected plasmin susceptibility. In the presence of calcium, we obtained the same pattern of results that were obtained without added calcium. Natural plasma gelsolin was cleaved into a 70 kDa fragment and recombinant into a 65 kDa fragment (Figure 1, lanes i and k). In contrast, both forms were converted into a 70 kDa form by plasmin in the presence of EDTA (compare lanes m and o). The difference in proteolytic susceptibility in the presence of calcium or EDTA indicates that the 65 kDa cleavage site is only exposed in the calcium-dependent conformation. The calcium dependence was further evaluated by first treating the samples with EDTA and then adding excess calcium and testing them for proteolytic susceptibility. Under these conditions, natural gelsolin generated the 70 kDa fragment and recombinant the 65 kDa fragment (data not shown), supporting this notion. The formation of the 65 kDa adduct in the absence of added calcium presumably reflects the fact that the gelsolin had been treated with calcium at the later stage of purification and therefore was already in the appropriate state.

The 65 and 70 kDa bands were further characterized by N-terminal sequencing. The sequence for the 70 kDa band was HVVPNEVVVQRLFQV starting at His^{151} in the plasma gelsolin sequence, while the sequence of the 65 kDa fragment was ARVHVSEEGTEPEAM starting at Ala^{229}. The spacing between the cleavage sites and the relevant Cys residues spans 78 amino acids, indicating that a substantial segment of domain 2 is affected by the formation of the disulfide. Other proteases that had been tested, including V8 protease, trypsin, and endo Lys-C, produced a similarly sized 65 kDa fragment for recombinant gelsolin under limiting digestion conditions that was not detected with natural plasma gelsolin, supporting the notion that the structural perturbation to domain 2 is substantial. The results with plasmin were particularly striking, since plasmin seemed to target a single site albeit different in the two gelsolin preparations.

Similar studies were performed on recombinant human plasma gelsolin that had been produced in Cos cells. The secreted gelsolin was indistinguishable from natural gelsolin. On the basis of the peptide mapping analysis, over 92% of the product contained the Cys^{188}−Cys^{201} disulfide (see Table 3). By limited proteolysis with plasmin, the Cos-derived and natural gelsolin generated the same pattern of cleavage products; i.e., the 70 kDa band formed under all conditions (see Figure 1).

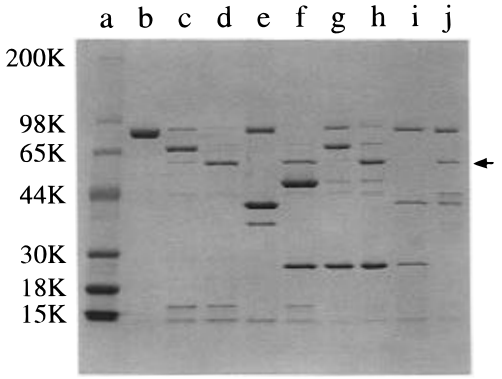

FIGURE 7: Assessing the proteolytic susceptibility of glutathione-oxidized recombinant gelsolin and platelet-derived cytoplasmic gelsolin to digestion with plasmin. The samples indicated below were treated with plasmin at an enzyme to gelsolin ratio of 1:10 in calcium-containing buffer as described in Experimental Procedures. Cleavage products were subjected to SDS−PAGE on a 4−20% gradient gel and visualized with Coomassie blue. Recombinant human plasma gelsolin from *E. coli* was plasmin digested directly (lane d) or after the following treatments: an 8-fold molar excess of F-actin (lane e), a 6-fold molar excess of 2C4 antibody in solution (lane f), and immobilization on 2C4-Sepharose (lane h). Recombinant human plasma gelsolin produced in *E. coli* that had been oxidized with glutathione was analyzed directly (lane b), digested with plasmin in solution and analyzed (lane c), or immobilized on 2C4 CNBr−Sepharose and digested with plasmin (lane g). Natural human cytoplasmic gelsolin from platelets was immobilized on 2C4-Sepharose and then analyzed with (lane j) or without digestion with plasmin (lane i). Lane a, prestained molecular weight markers from Gibco BRL. The positions of molecular weight standards are indicated at the left of the figure. The arrowhead at the right marks the position of the 65 kDa cleavage fragment. Prominent bands at 42 kDa in lanes e, i, and j, at 55 kDa in lane f, and at 25 kDa in lanes f−i correspond to actin, IgG heavy chain, and IgG light chain, respectively.

Platelet-derived cytoplasmic gelsolin was also tested for susceptibility to proteolysis with plasmin. As shown in lane j of Figure 7, only the 65 kDa cleavage product was observed after treatment with plasmin, indicating that this feature of cytoplasmic gelsolin structure resembles recombinant gelsolin produced in *E. coli*.

Formation of the Correct Disulfide after Treatment with Oxidized Glutathione. Since recombinant gelsolin from *E. coli* lacked the intradomain 2 disulfide, we tested if the disulfide could be induced to form by mild oxidation. Using

peptide mapping to monitor disulfide formation, we achieved the desired result. After an 18 h incubation with 2 mM oxidized glutathione, over 95% of the product contained the $Cys^{188}-Cys^{201}$ disulfide. The other Cys residues were not affected by the oxidation step. The glutathione-oxidized gelsolin produced the 70 kDa fragment in the proteolysis assay with plasmin when run in the presence of calcium (Figure 7, lane c), indicating that the absence of the disulfide and the structural differences detected by limited proteolysis were related. Forty-two percent of the disulfide formed in parallel samples that had been incubated without the addition of glutathione (see Table 3). While the free thiols were readily susceptible to oxidation, we were unable to reverse the process by reduction. Treatment of natural plasma gelsolin with 0.2 mM DTT had no effect on the oxidation state.

DISCUSSION

We have developed a peptide mapping/mass spectrometric strategy that was used to analyze the disulfide structure of gelsolin. With this method, we demonstrated that all five of the Cys residues in cytoplasmic gelsolin are in the free thiol form, while only three of the five thiols in plasma gelsolin are free. In plasma gelsolin, an intradomain disulfide links Cys^{188} and Cys^{201}. The mapping results provide the first definitive evidence that the cytoplasmic and plasma forms of gelsolin are structurally distinct. Although both forms of gelsolin have been known for over a decade, there is little published information on potential differences between them. Our data highlight the need for more rigorous tests of function. Interestingly, in the one published study where natural and recombinant plasma and cytoplasmic forms of human gelsolin were characterized by microinjection for their effects on stress fiber networks (Huckriede et al., 1990), only the natural plasma gelsolin was active, suggesting that functional differences may exist. The mapping method, which takes advantage of the peak absorbance of PE-Cys at 254 nm, is a useful tool for monitoring the structure of gelsolin and should be readily applicable to other proteins.

In addition, the disulfide structures of two recombinant versions of human plasma gelsolin that had been expressed intracellularly in *E. coli* and as a secreted protein from Cos cells were also characterized. The *E. coli*-derived gelsolin lacked the disulfide while the mammalian product contained the correct disulfide. Disulfide formation in the *E. coli* product could be induced by mild oxidation. Without added oxidant, disulfide formation occurred at a reduced rate. Calcium was needed for the oxidation to occur (data not shown), though the mechanism by which calcium catalyzed disulfide formation was not investigated. The present data indicate that the *E. coli*-derived gelsolin product is not a true mimic of natural plasma gelsolin but instead more closely resembles cytoplasmic gelsolin. Since recombinant forms of plasma gelsolin from *E. coli* are routinely used by other laboratories to study structure/function, it will be important to determine the oxidation state of these products.

Differences in structure were also apparent when samples were tested by limited proteolysis with plasmin. The *E. coli*-derived recombinant gelsolin and cytoplasmic gelsolin from platelets were cleaved into a 65 kDa fragment, while natural plasma gelsolin and the Cos-derived product were cleaved into a 70 kDa form. N-Terminal sequence data revealed that the 70 kDa fragment resulted from cleavage at the domain 1−2 interface and that the 65 kDa fragment resulted from cleavage within domain 2. The differences in proteolytic susceptibility disappeared upon formation of the disulfide bond. Thus the process of forming the disulfide must promote the changes in domain 2 structure that are detected by proteolysis. We infer that the domain 2 specific differences seen between recombinant gelsolin from *E. coli* and natural plasma gelsolin are analogous to differences between cytoplasmic and plasma gelsolin.

While the cleavage data for cytoplasmic gelsolin clearly reveal the 65 kDa fragment, the analysis was complicated by the presence of actin in the preparation. Preliminary tests revealed that the actin−gelsolin complex was resistent to proteolysis presumably because actin binding blocked the sites that are susceptible to digestion when gelsolin is in the free state (see Figure 7, lane e). A method for cleavage was developed using 2C4-Sepharose to collect and wash the gelsolin prior to digestion. Immobilization on the 2C4 antibody had no impact on the ability to cleave gelsolin with plasmin (see Figure 7). Even with these modifications, only about 30% of the cytoplasmic gelsolin was cleaved. While several groups have developed strategies for separating platelet gelsolin from actin, these methods rely on the addition of denaturants or chaotropes to dissociate the complexes which were not considered to be appropriate for our analysis (Olomucki et al., 1984; Weeds et al., 1986) since the treatments themselves could perturb structure. In these studies activity alone was used as an indicator for correct folding.

The three-dimensional structures of gelsolin domain 1 and villin domain 1 are highly homologous (Markus et al., 1994). By assuming that the tertiary structures of the other gelsolin domains also are homologous, and using domain 1 of villin as a model for their structure, we found that Cys^{188} and Cys^{201} in domain 2 and Cys^{304} in domain 3 are buried and Cys^{93} in domain 1 and Cys^{645} in domain 6 are in loop structures. On the basis of the model, the distance between the α-carbons of Cys^{188} and Cys^{201} is 4−5 Å, which is close enough to accommodate the disulfide without invoking the need for a large conformational change (Figure 8). The spacial orientation of the plasmin cleavage sites was also investigated. Both the His^{151} and Ala^{229} cleavage sites are far removed from the relevant Cys residues (Figure 8). The fact that the His^{151} and Ala^{229} cleavage sites are influenced by oxidation despite the relatively large distance between the relevant amino acids indicates that a large segment of domain 2 is affected by the formation of the disulfide (see Figure 8).

Recently, Schnuchel et al. (1995) determined the NMR structure of severin domain 2 and noted the presence of a disulfide in the structure. In this case, however, the disulfide bond is between Cys^{189}, which is homologous to Cys^{188} in gelsolin, and Cys^{235}, which is not homologous to a Cys residue in gelsolin. In gelsolin the $Cys^{188}-Cys^{201}$ disulfide links β-strands 3 and 4, whereas in severin the $Cys^{189}-Cys^{235}$ disulfide links β-strands 3 and 5. When the villin structure is used as a template for modeling domain 2 of severin, Cys^{189} and Cys^{235} (denoted with green circles in Figure 8) are separated by approximately 10 Å, and when the severin structure is used as a template for domain 2 of gelsolin, the α-carbon distance between Cys^{188} and Cys^{201} is about 3 Å (data not shown). Since a 5−6 Å α-carbon distance is

FIGURE 8: Apparent features of domain 2 of gelsolin based on the villin structure. The previously published NMR structure of domain 1 from villin (Markus et al., 1994) was used as a model for domain 2 of gelsolin. Residue numbers 145 and 264 indicate the sequence orientation. The positions of the relevant amino acids Cys^{188}, Cys^{201}, His^{151}, and Ala^{229} are indicated. Apparent distances between His^{151} and Cys residue 188 or 201 and between Ala^{229} and Cys residue 188 or 201 ranged from 17 to 20 Å. The apparent distance between His^{151} and Ala^{229} was 16 Å. Green circles denote the relative positions of the Cys residues from domain 2 of severin that are disulfide linked.

typically needed to accommodate a disulfide, neither model can accommodate both the Cys^{188}−Cys^{201} and the Cys^{189}−Cys^{235} disulfides simultaneously without invoking a conformational change. While it is likely that both types of disulfides can stabilize the tertiary structure of their respective domains, the data indicate a certain degree of flexibility in the overall structure of domain 2. The failure of the models to accommodate all of the structural data highlights the need for a more detailed analysis of the structure of domain 2 of gelsolin.

The presence of the disulfide in the solution structure of domain 2 of severin is surprising. The *Dictyostelium* cytoplasm, like the mammalian intracellular milieu, is a reducing environment, and therefore one would predict that the Cys residues in severin would be in a free state. Since there is no information on the oxidation state of the cysteines in severin, it is unclear if the domain 2 structure mimics severin or reflects an unnatural state. Further studies are needed to test this point. The experiments we performed with cytoplasmic gelsolin point out the difficulties of this type of analysis and should form a framework for these studies. While mild oxidation could convert gelsolin from a reduced to an oxidized state, the disulfide-linked form was resistant to reduction without prior denaturation of the gelsolin. Whether this observation reflects the fact that the relevant Cys residues are buried and inaccessible to the reductant or that the disulfide-linked form is a more stable conformation remains to be determined.

In the hereditary disease known as gelsolin-induced amyloidosis, Finnish type, an Asp^{187} to Asn^{187} point mutation in domain 2 of gelsolin renders the protein sensitive to proteolysis. No intact gelsolin is present in the serum from individuals carrying this defect, but instead a *ca*. 65 kDa fragment of gelsolin is observed that is missing residues 1−172 (Maury & Rossi, 1993). Weeds and co-workers (1993) have speculated that the point mutation prevents the formation a salt bridge between Asp^{187} and Arg^{169} and that this leads to the observed instability. Since Asp^{187} is next to Cys^{188}, we propose that the mutation blocks disulfide formation and that the abnormal susceptibility to proteolysis may be related to the structural effects we characterized. In our model, the resulting free thiol groups at Cys^{188} and Cys^{201} would then be available for disulfide-mediated aggregation, and this leads to the buildup of the Ala^{173}−Met^{243} fragment in the amyloid plaque. It will be interesting to test our model by determining the disulfide structure of the 65 kDa fragment of the mutant form. The unexpected phenotype of the point mutation further highlights the significance of this segment of the gelsolin sequence. The studies we performed here, which demonstrate that the plasma and cytoplasmic forms of gelsolin are structurally distinct, provide a series of useful methods for evaluating gelsolin structure. These studies should form the basis for future work targeted at assessing the effect of the changes in structure on structure/function.

ACKNOWLEDGMENT

We thank Celine Grunt for providing bacteria expressing gelsolin and Carmen Young and Paul Courchesne for N-terminal sequence data. We also thank Phil Allen, Tom Stossel, and Susan Goelz for helpful discussions, and Joe Rosa and Alphonse Galdes for critical reading of the manuscript.

REFERENCES

Ankenbauer, T., Kleinsohmidt, J. A., Vanderkerckhove, J., & Franke, W. W. (1988) *J. Cell Biol. 107*, 1489−1498.
Bazari, W. L., Matsudaira, P., Wallek, M., Smeal, T., Jakes, R., & Ahmed, Y. (1988) *Proc. Natl. Acad. Sci. U.S.A. 85*, 4986−4990.
Chaponnier, C., Janmey, P. A., & Yin, H. L. (1986) *J. Cell Biol. 103*, 1473−1481.
Creighton, T. E. (1990) in *Protein structure: a practical approach* (Creighton, T. E., Ed.) pp 157−158, IRL Press, Oxford.
Dieffenbach, C. W., SenGupta, D. N., Krause, D., Sawzak, D., & Silverman, R. H. (1989) *J. Biol. Chem. 264*, 13281−13288.
Heintzelman, M. B., Frankel, S. A., Artavanis-Tsakonas, S., & Mooseker, M. S. (1993) *J. Mol. Biol. 230*, 709−716.
Huckriede, A., Fuchtbauer, A., Hinssen, H., Chaponnier, C., Weeds, A., & Jockusch, B. M. (1990) *Cell Motil. Cytoskel. 16*, 229−238.
Hwang, C., Sinskey, A. J., & Lodish, H. (1992) *Science 257*, 1496−1502.
Janmey, P. A. (1995) *Curr. Biol. (Chem., Biol.) 2*, 61−65.
Kilhoffer, M. C., & Gerard, D. (1985) *Biochemistry 24*, 5653−5660.
Kurokawa, H., Fujii, W., Ohmi, K., Sakurai, T., & Nonomura, Y. (1990) *Biochem. Biophys. Res. Commun. 168*, 451−457.
Kurth, M. C., & Bryan, J. (1984) *J. Biol. Chem. 259*, 7473−7479.
Kwiatkowski, D. J., & Yin, H. L. (1989) *Cell Motil. Cytoskel. 14*, 21−25.
Kwiatkowski, D. J., Stossel, T. P., Orkin, S. H., Mole, J. E., Coten, H. R., & Yin, H. L. (1986) *Nature 323*, 455−458.
Kwiatkowski, D. J., Mehl, R., & Yin, H. L. (1988) *J. Cell Biol. 106*, 375−384.
Kwiatkowski, D. J., Janmey, P. A., & Yin, H. L. (1989) *J. Cell Biol. 108*, 1717−1726.
Lueck, A., d'Haese, J., & Hinssen, H. (1994) *EMBL Data Library*, Accession S41391.
Markus, M. A., Nakayama, T., Matsudaira, P., & Wagner, G. (1994) *Protein Sci. 3*, 70−81.
Maury, C. P. J., & Rossi, H. (1993) *Biochem. Biophys. Res. Commun. 191*, 41−44.
McLaughlin, P. J., Gooch, J. T., Mannherz, H.-G., & Weeds, A. G. (1993) *Nature 364*, 685−692.
Olomucki, A., Hue, C., Lefebure, F., & Coue, M. (1984) *FEBS Lett.* 174, 80−85.
Pepinsky, R. B. (1991) *Anal. Biochem. 195*, 177−181.
Pope, B., Maciver, S., & Weeds, A. (1995) *Biochemistry 34*, 1583−1588.
Reid, S. W., Koepf, E. K., & Burtnick, L. D. (1993) *Arch. Biochem. Biophys. 302*, 31−36.

Schnuchel, A., Wiltscheck, R., Eichinger, L., Schleicher, M., & Holak, T. A. (1995) *J. Mol. Biol. 247*, 21−27.
Stossel, T. P., Chaponnier, C., Ezzell, R., Hartwig, J. H., Janmey, P., Kwiatkowski, D. J., Lind, S. E., Smith, D. B., Southwick, F. S., Yin, H. L., & Zaner, K. S. (1985) *Annu. Rev. Cell Biol. 1*, 353−402.
Vasconcellos, C. A., Allen, P. G., Wohl, M. E., Drazen, J. M., Janmey, P. A., & Stossel, T. P. (1994) *Science 263*, 969−971.
Wang, L. L., & Bryan, J. (1981) *Cell 25*, 637−649.
Way, M., & Weeds, A. (1988) *J. Mol. Biol. 203*, 1127−1133.
Way, M., Gooch, J., Pope, B., & Weeds, A. (1989) *J. Cell Biol. 109*, 593−605.
Weeds, A., & Maciver, S. (1993) *Curr. Opin. Cell Biol. 5*, 63−69.
Weeds, A. G., Gooch, J., Pope, B., & Harris, H. E. (1986) *Eur. J. Biochem. 161*, 69−76.
Weeds, A. G., Gooch, J., McLaughlin, P., & Maury, C. P. J. (1993) *FEBS Lett. 335*, 119−123.
Witke, W., Sharpe, A. H., Hartwig, J. H., Azuma, T., Stossel, T. P., & Kwiatkowski, D. J. (1995) *Cell 81*, 41−51.
Yin, H. L. (1987) *Bioassays 7*, 176−179.
Yin, H. L., & Stossel, T. P. (1979) *Nature 281*, 583−586.

BI960920N